UC Berkeley
Working Papers

Title
A Time Headway Autonomous Intelligent Cruise Controller: Design and Simulation

Permalink
https://escholarship.org/uc/item/68v505tv

Authors
Ioannou, P.A.
Ahmed-Zaid, F.
Wuh, D.H.

Publication Date
1994-04-01

eScholarship.org Powered by the California Digital Library
University of California

This paper has been mechanically scanned. Some errors may have been inadvertently introduced.

CALIFORNIA PATH PROGRAM
INSTITUTE OF TRANSPORTATION STUDIES
UNIVERSITY OF CALIFORNIA, BERKELEY

A Time Headway Autonomous Intelligent Cruise Controller: Design and Simulation

P.A. Ioannou, F. Ahmed-Zaid, D.H. Wuh

University of Southern California

California PATH Working Paper

UCB-ITS-PWP-94-07

This work was performed as part of the California PATH Program of the University of California, in cooperation with the State of California Business, Transportation, and Housing Agency, Department of Transportation.

The contents of this report reflect the views of the authors who are responsible for the facts and the accuracy of the data presented herein. The contents do not necessarily reflect the official views or policies of the State of California. This report does not constitute a standard, specification, or regulation.

April 1994

ISSN 1055-1417

A Time Headway Autonomous Intelligent Cruise Controller: Design and Simulations*

P.A. Ioannou, F. Ahmed–Zaid and D. H. Wuh

Southern California Center for

Advanced Transportation Technologies

EE - Systems, EEB 200B

University of Southern California

Los Angeles, CA 90089-2562

Abstract. Autonomous Intelligent Cruise Control (AICC) design is an important part of Advanced Vehicle Control Systems (AVCS). In this report, we design an AICC scheme for vehicle following with constant time headway spacing. The scheme maintains a steady state inter–vehicle spacing decided by a desired time headway set by the driver. The longitudinal model of the Lincoln Town Car is used for simulations and testing. The vehicle is assumed to be equipped with a relative distance and speed measuring sensor, as well as an absolute speed measuring device.

1 Introduction

In this report, we focus on an important aspect of Advanced Vehicle Control Systems, namely, the design of Autonomous Intelligent Cruise Controllers [1]. The objective of the design is vehicle following under constant time headway policy. The controller is designed to achieve steady state vehicle spacing for a preselected time headway. Driving comfort constraints such as a low acceleration at high speeds and a minimum amount of jerk, as well as a limited throttle angle rate of change and throttle actuator delay are taken into account.

The longitudinal vehicle model of the Lincoln Town car is used in this study. We consider the case of one vehicle following a lead car and assume that the former is equipped with a relative distance and speed measuring sensor, as well as a speed measuring device of its velocity. The design is based on the use of the inverse mapping, which is assumed to exist, between the acceleration and the throttle angle. Following this approach, we are able to

*This work is supported by Caltrans through PATH of University of California and Ford Motor Company.

simplify the control design to achieve our objective. During the design phase, we take into account the imperfection of the inverse mapping and load disturbances, and implement a feature for rejecting their effects on the overall system performance.

Simulations illustrating the performance of the proposed controller are included for a wide range of velocities, along with results for constant load disturbances and varying time headway.

2 Longitudinal Vehicle Model

The longitudinal vehicle model is shown in Fig. 1. Only some of the important inputs and

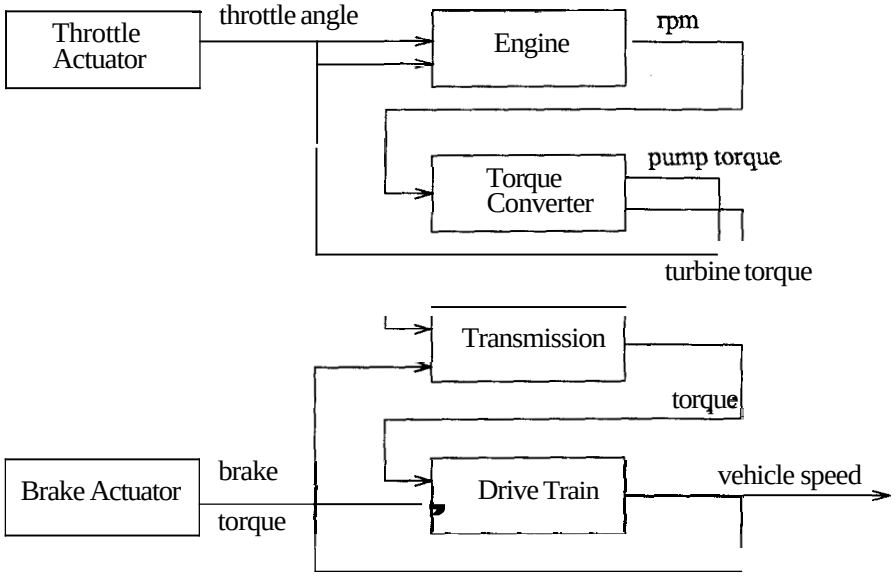

Figure 1: Longitudinal Vehicle Model.

outputs are included in the figure. The six main components of the longitudinal vehicle model are the engine, the torque converter, the transmission, the drive train and the throttle and brake actuators. The external input to the model is the throttle angle and brake torque. The primary output is the vehicle speed.

The engine model includes manifold filling and induction lag dynamics, so that the transient response of the engine is reasonably well represented. Fig. 2 shows a simplified form of the engine model. The throttle map provides an air mass flow rate $\dot{m}_{out}$ into the engine as

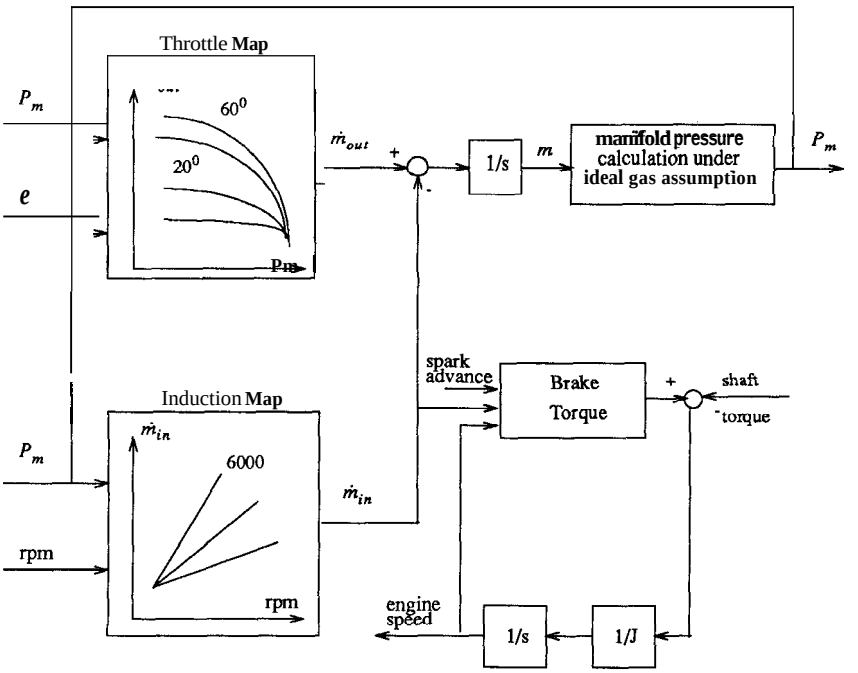

Figure 2: Simplified Engine Model.

a function of throttle angle θ and manifold pressure P_m. The characteristics of the throttle map are shown in the figure. The induction map describes engine pumping characteristics and generates an air mass flow rate $\dot{m}_{in}$ as a function of engine rpm and manifold pressure. After obtaining the fuel mass m, this mass change is then used for calculating the manifold pressure under the assumption of ideal gas. The engine brake torque, which is the combustion torque minus the friction loss torque, is implemented in this model in the form of tables based on experimental data. The difference between brake torque and total load torque (engine shaft torque) is then used to compute the engine speed according to Newton's law.

In the torque converter model, the turbine torque is calculated by multiplying the engine torque together with the torque ratio. The latter is a nonlinear function of the ratio between turbine and engine speeds. The engine torque is proportional to the square of the engine speed, with the proportionality term being the capacity factor, which is a nonlinear function of the speed ratio between the engine speed and the transmission.

The transmission model determines gear shifting based upon vehicle speed and throttle angle. First, the percent wide open throttle shift point is determined based on vehicle speed.

Then, the throttle angle is checked for shifting. After gear selection is determined, a simple first order filter is used to provide a smooth gear transition.

In the drive train model, rear axle gear and single mass vehicle are considered. Therefore the ideal wheel torque contributes to push the vehicle forward, and the windage drag acts in the opposite direction.

In the throttle actuator model, the pure time delay is taken to be 0.2 seconds, and slew rate is considered to be 40 degrees per second. The brake actuator is modeled as a pure delay along with a first order lag.

2.1 Throttle Model

The model of the vehicle dynamics described in the previous section is summarized by the following figure

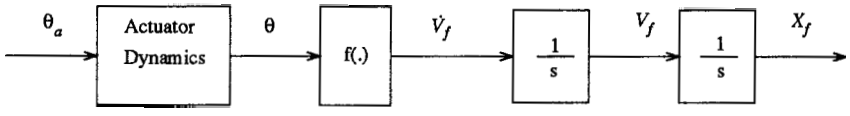

Figure 3: Model of Vehicle Dynamics.

where

θ : throttle angle in degrees

$\dot{V}_f$: acceleration in m/s^2

V_f : vehicle velocity in m/s

X_f : absolute position in m

$f(\cdot)$: nonlinear mapping from θ to $\dot{V}_f$

Control Objective:

Choose θ so that V_f follows V_l, the velocity of the lead vehicle, and the intermediate spacing S (measured from the front of the following vehicle to the rear of the leading vehicle) satisfies

$$S = hV_f + S_0 \tag{2.1}$$

where h is the time headway in seconds and $S_0 \geq 0$ is a constant spacing for additional safety distance.

The control objective has to be achieved under the following constraints

c1. For 30mph $\leq V_f \leq$ 50 mph, $\dot{V}_f$ should satisfy $-0.15g \leq \dot{V}_f \leq 0.07g$
For $V_f >$ 50 mph, $\dot{V}_f$ should satisfy $-0.15g \leq \dot{V}_f \leq 0.05g$
where g $= 9.81 m/s^2$.

c2. $|\dot{\theta}| \leq$ 40 deg/s and $0 \leq 8 \leq$ 80 deg

c3. The jerk $|\dddot{V}_f|$ should be **as** small as possible.

3 Controller Structure: Inverse Mapping Approach

In this approach, the control problem is simplified by assuming that the inverse mapping $f^{-1} : \dot{V}_f \longrightarrow \theta$ exists and can be calculated on line. The throttle θ is chosen **as**

$$\theta = f^{-1}(u) \tag{3.1}$$

where u is another input and $\hat{f}^{-1}(\cdot)$ is an approximation of $f^{-1}(\cdot)$. The discrepancy between $\hat{f}^{-1}$ and f^{-1} may be modeled as

$$\hat{f}^{-1}(u) = f^{-1}(u) + d_f \tag{3.2}$$

where d_f can be treated **as** a bounded disturbance.

Using **(3.2)** and neglecting the actuator dynamics, the vehicle model is represented by Figure **4**

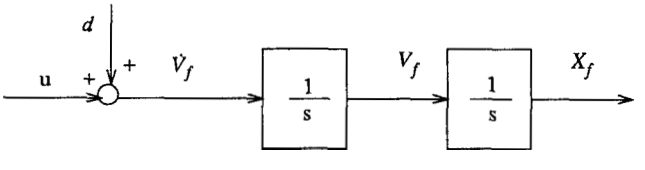

Figure 4: Simplified Vehicle Model.

where d $= f(d_f)$ is treated as a bounded disturbance, and u is the input to be selected. The control input u has the same units as $\dot{V}_f$. When $d = 0$, u can be treated **as** the desired

acceleration the vehicle has to undergo in order to meet the control objective. The value of the throttle angle 8 is obtained through the inverse mapping **(3.1)** as follows: from u, we calculate the required wheel torque which is then used to compute the engine torque through the inverse form of the transmission and the engine map. The inverse transmission model calculates the required engine torque according to the gear ratio. The engine torque and rpm are then used in the inverse engine map to determine the required throttle angle 8. We neglect the manifold and torque converter dynamics since they mainly affect the transient response.

We now use the above model to choose u to achieve the control objective. Since the only unknown in the model is d no parameter estimation is required.

The controller structure based on the simplified model takes the form given in Figure 5.

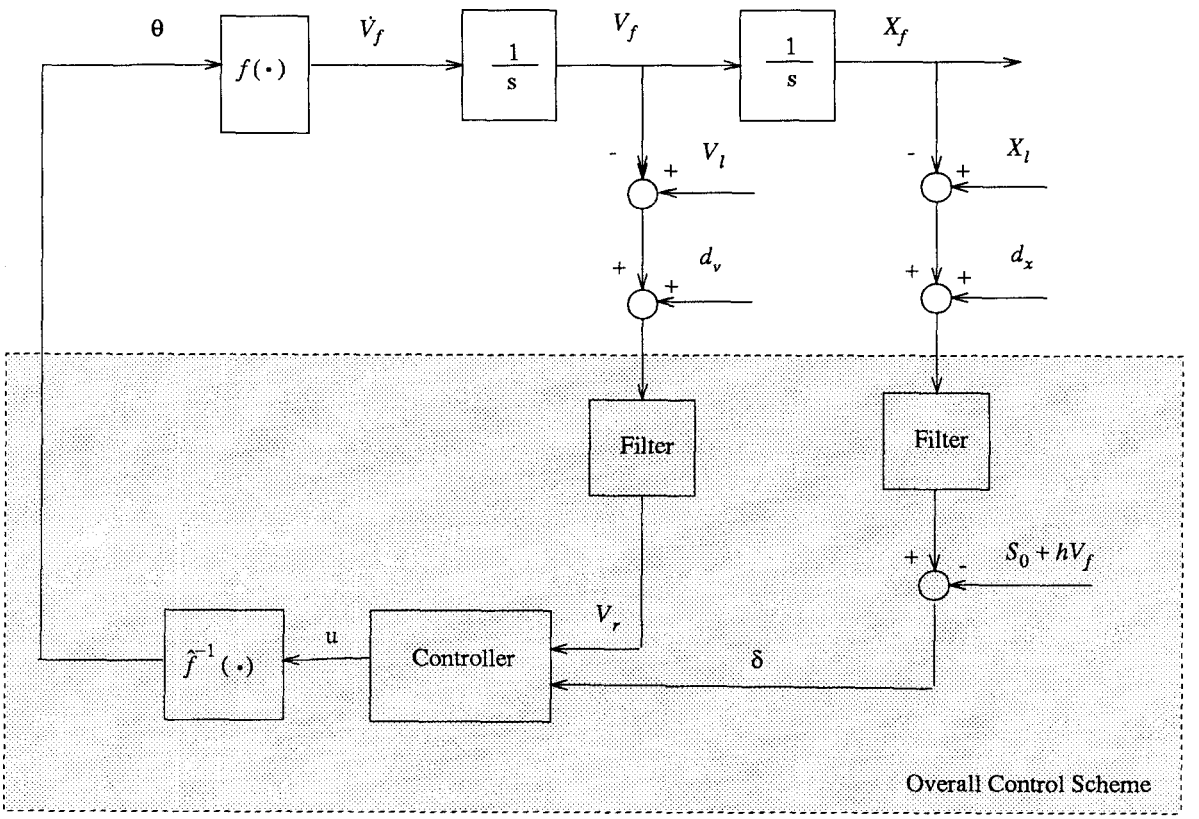

Figure 5: Overall Throttle Control System.

- d_v, d_x: denote the measurement noise due to relative distance and speed sensor
- Filter: Denotes filtering of the measurements to attenuate the noise effects.

A wide class of controllers can now be designed and used with the above structure. We propose the following simple controllers:

3.1 Controller A: PID control

Let δ be the deviation from the desired spacing $S = hV_f + S_0$, i.e.

$$\delta = X_l - X_f - hV_f - S_0$$

and let [illegible] be the relative velocity error

$$[illegible] = V_l - [illegible]$$

We propose the following control law

$$u = -k_1\delta - k_2V_r - k_3\frac{1}{s}\delta = -(k_1 + \frac{k_3}{s})\delta - k_2V_r$$

where k_1, [illegible] k_3 are the controller gains to be calculated.

The vehicle model shown in Figure **4** may be represented as

$$\dot{V}_f = d + u$$

$$X_f = v_f$$

In terms of δ, [illegible] we have

$$\dot{\delta} = V_r - h\dot{V}_f = V_r - hd - hu$$

$$\dot{V}_r = -d - u + \dot{V}_l$$

or, equivalently,

$$\delta = \frac{1}{s}(V_r - hu) - \frac{1}{s}hd$$

$$[illegible] = -\frac{1}{s}u - \frac{1}{s}d + \frac{1}{s}\dot{V}_l$$

Substituting for u, we obtain the following transfer functions

$$\delta = \frac{(1 + hk_2)s^2}{[illegible] - (k_2 + hk_1)s^2 - (k_3h + k_1)s - k_3}V_l - \frac{(1+hs)s}{s^3 - (k_2 + hk_1)s^2 - (k_3h + k_1)s - k_3}d$$

$$V_r = \frac{(s^2 - hk_1 s - hk_3)s}{s^3 - (k_2 + hk_1)s^2 - (k_3 h + k_1)s - k_3} V_l - \frac{s^2}{s^3 - (k_2 + hk_1)s^2 - (k_3 h + k_1)s - k_3} d$$

The gains k_1, k_2 and k_3 can now be chosen so that the poles of the above transfer functions are at selected locations within the left half s-plane.

If d is constant, or slowly time-varying, we will have $sd \simeq 0$ and d will have no or little effect on δ and V,.

Similarly, if $\dot{V}_l$ is a constant or varies slowly, it will have little or no effect on δ. $\dot{V}_l$ will however cause V_r to be nonzero, in other words, during high acceleration or high deceleration of the leading vehicle, the **PID** controller may not achieve good velocity tracking.

Let us now choose k_1, k_2, k_3 so that

$$s^3 - (k_2 + hk_1)s^2 - (k_3 h + k_1)s - k_3 = (s + \lambda_0)(s_2 + 2\zeta\omega_n s + \omega_n^2) \tag{3.3}$$

where $-\lambda_0$ is a desired pole and ω_n, ζ are the natural frequency and damping ratio, respectively, of the two complex roots. The values of ζ, w, and λ_0 are chosen to shape the response of δ, V_r and meet the constraints (**c1**–**c3**) as close as possible.

From **(3.3)** we obtain

$$\begin{aligned} k_1 &= -(1 - \lambda_0 h)\omega_n^2 - 2\zeta\omega_n\lambda_0 = -2\zeta\omega_n\lambda_0 - \omega_n^2 + \lambda_0\omega_n^2 h \\ k_2 &= -\lambda_0 - (1 - h\lambda_0)(2\zeta - h\omega_n)\omega_n = -\lambda_0 - 2\zeta\omega_n + h(\omega_n^2 + 2\lambda_0\zeta\omega_n) - h^2\lambda_0\omega_n^2 \\ k_3 &= -\lambda_0 - w^2 \end{aligned}$$

By selecting desired values for ζ, ω_n and λ_0, we can easily obtain expressions for the gains k_i, $i = 1, 2, 3$ as functions of the time headway h. These gains are then tuned through simulations to satisfy the constraints (**c1**–**c3**).

3.2 Controller B: Linear Quadratic (LQ) control

Another design approach followed in this study is the linear quadratic control methodology. The controller gains in this case are calculated by minimizing a preselected cost function depending on the quantities that we wish to minimize, along with various weightings to be chosen appropriately. For design purposes, similarly as in the case of the **PID** controller, the

vehicle model is taken as

$$\begin{aligned} \dot{\delta} &= V_r - hu - hd \\ \dot{V}_r &= -u - d + \dot{V}_l \end{aligned}$$

By introducing the integral position error $z_1 = \int_0^t \delta(\tau)d\tau$ as an additional state to be used for the control design, we can rewrite the system as

$$\begin{bmatrix} \dot{z}_1 \\ \dot{\delta} \\ \dot{V}_r \end{bmatrix} = \begin{bmatrix} 0 & 1 & 0 \\ 0 & 0 & 1 \\ 0 & 0 & 0 \end{bmatrix} \begin{bmatrix} z_1 \\ \delta \\ V_r \end{bmatrix} + \begin{bmatrix} 0 \\ -h \\ -1 \end{bmatrix} u + \begin{bmatrix} 0 \\ -h \\ -1 \end{bmatrix} d + \begin{bmatrix} 0 \\ 0 \\ 1 \end{bmatrix} \dot{V}_l \tag{3.4}$$

or equivalently,

$$\dot{z} = Az + bu + bd + b_1\dot{V}_l$$

where

$$z = [z_1,\ \delta,\ V_r]^T;\quad A = \begin{bmatrix} 0 & 1 & 0 \\ 0 & 0 & 1 \\ 0 & 0 & 0 \end{bmatrix};\quad b = \begin{bmatrix} 0 \\ -h \\ -1 \end{bmatrix};\quad b_1 = \begin{bmatrix} 0 \\ 0 \\ 1 \end{bmatrix}$$

The introduction of the new state $z_1 = \int_0^t \delta(\tau)d\tau$, is necessary in the control design in order to be able to cancel any steady state error due to modeling or load disturbances.

As a criterion for control design, we select the following cost function

$$J = \int_0^\infty [z(\tau)^T Q z(\tau) + \lambda u^2(\tau)]d\tau$$

subject to the constraint

$$\dot{z} = Az + bu \tag{3.5}$$

The cost function J consists of integrals of quadratic forms of quantities we wish to minimize, namely, integral position and position errors (z_1 and δ respectively), relative velocity error and control action (V_r and u respectively). The quantities Q and X represent the weighting factors penalizing the system state z and the control input u. The weighting matrix Q is of

the form

$$Q = \begin{vmatrix} q_1 & 0 & 0 \\ 0 & q_2 & 0 \\ 0 & 0 & q_3 \end{vmatrix}$$

where $q_1 > 0$ penalizes the integral position error in the cost J, $q_2 > 0$ penalizes the position error and $q_3 > 0$ penalizes the relative velocity error. q_1 is to be chosen relatively small compared to q_2, q_3 since we wish to penalize the position error and the control action more than the other errors. **A** typical choice for Q, X would be

$$Q = \begin{bmatrix} 0.01 & 0 & 0 \\ 0 & 1 & 0 \\ 0 & 0 & 0.1 \end{bmatrix} \text{ and } \lambda = 10$$

For a fixed time headway, after selecting the weightings Q and X, the LQ control input is given by

$$u = -Kz = -\lambda^{-1} b^T P z$$

where P, is the solution to the algebraic Ricatti equation

$$A^T P + PA - Pb\lambda^{-1} b^T P + Q = 0$$

The feedback gain K is computed for different headway values $h = 0.6,\ 0.8,\ \ldots,\ 1.8,\ 2.0$ seconds and implemented in (3.4) for a constant disturbance, d = 0.01 g for instance, $\dot{V}_l = 0.3\sin(0.1t)$ and non–zero initial conditions, e.g. $z_1(0) = 0,\ x_1(0) = 40m,\ x_2(0) = 20\text{mph}$. The weightings Q and X are adjusted iteratively to satisfy the constraints (**c1–c3**). For different time headways, the calculated gains $k_i,\ i = 1, 2, 3$ are plotted in Figure 6. For the time headway range of interest, these gains are almost linear in h. The integral gain k_1, as in the PID case, is independent of the headway h. The two other gains ***kg,*** k_3 are slowly varying functions of h.

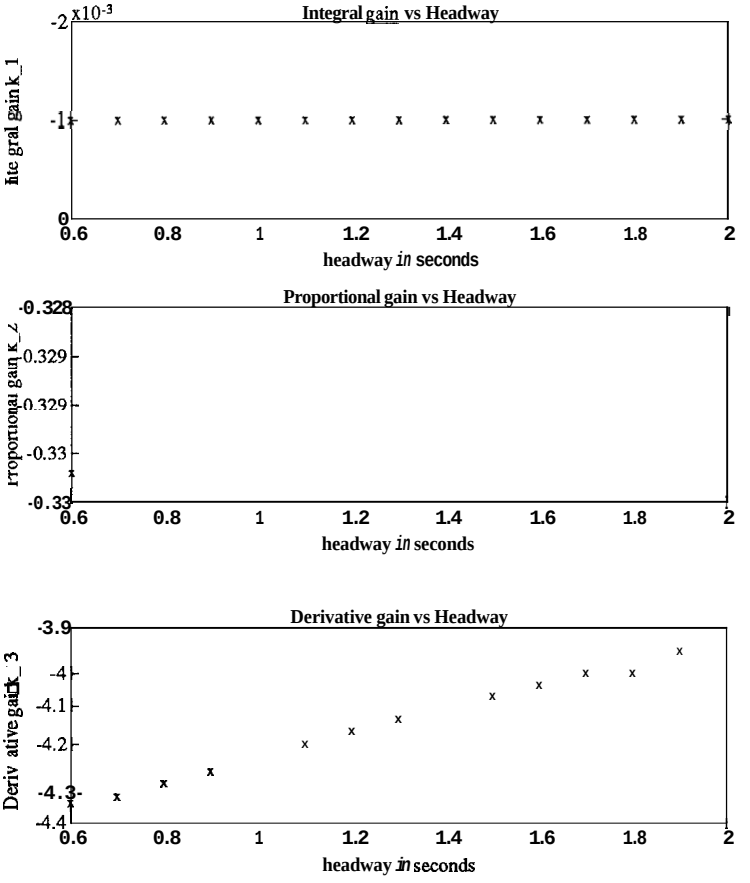

Figure 6: LQ/PID gains vs time headway.

4 Simulations

In order to satisfy the acceleration constraint (**c1.**), the actual leading vehicle velocity V_l is passed through a filter and acceleration limits before being used in the computation of the control input [2]. In other words, if the leading vehicle is accelerating at **a** much higher rate than the allowed acceleration for the following vehicle, the former is ignored and the controller provides the maximum allowed acceleration. **A** diagram illustrating this technique is shown in Figure 7(a).

Figure 7(b) is a block diagram of the PID/LQ controller implementation. Two limiters are used before feeding back the position error δ.

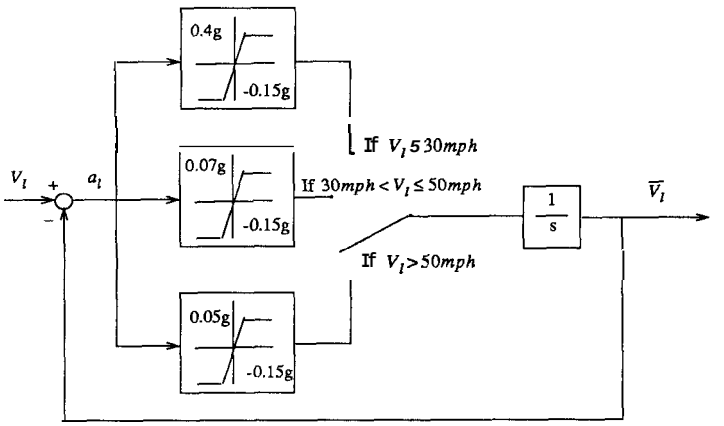

Figure 7: (a). Leading vehicle velocity filtering and acceleration limiting technique.

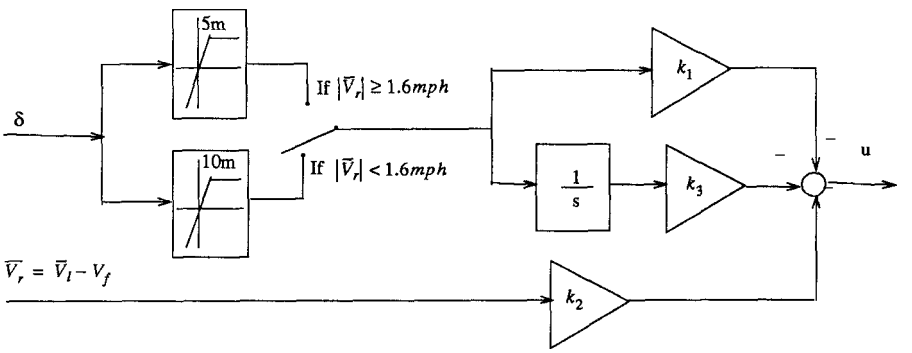

Figure 7: (b). PID and LQ controller implementation diagram.

A switch depending on the velocity error $\bar{V}_r = \bar{V}_l - V_f$ decides which limited position error δ will be fed into the PI section of the controller: in order to avoid feeding back large position error during the transient response ($|\bar{V}_r| \geq 1.6\,mph$), which will contribute to large accelerations, the signal used is δ limited to $5m$ in the positive direction. Once good velocity tracking is achieved, i.e. steady state is almost reached ($|\bar{V}_r| < 1.6\,mph$), then a higher position error through the feedback path is tolerated and in fact becomes the main contribution to the control input.

The integrator gain provides the necessary action for rejecting any constant load disturbances due to the inverse mapping imperfections or road inclines.

The following gains were selected for simulations:

PID controller: $k_1 = -0.3;\ k_2 = -4.0;\ k_3 = -0.0007$

PD controller: $k_1 = -0.3;\ k_2 = -4.0;\ k_3 = 0.0$

LQ controller: $k_1 = -0.33;\ k_2 = -4.22;\ k_3 = -0.001$

which were calculated using the following weighting factors:

$$Q = \begin{bmatrix} 10^{-5} & 0 & 0 \\ 0 & 1 & 0 \\ 0 & 0 & 200 \end{bmatrix} \text{ and } X = 10$$

4.1 Simulation results

- Test 1: High leading vehicle accelerations, time headway $h = 1$ second. See Figures 8(a) through 8(f).

Good velocity tracking is achieved, see Figure 8(a). The responses obtained with the PID and LQ controllers are quite similar. The accleration constraints are over all satisfied, and a zero steady error is achieved in the position error. The PD controller, however, exhibits a non–zero steady state error, as expected and illustrated in Fig. 8(c).

- Test 2: Constant load disturbance effects, time headway $h = 1$ second. See Figures 9(a) through 9(f).

Under a constant load disturbance, shown in Figure 9(f) and simulating an uphill road incline of about 4^0, good velocity tracking is achieved, see Figure 9(a). The steady state error in the position error for both the PID and LQ controllers is being driven to zero by the integral action, while satisfying the accleration constraints. The higher road incline and high speed $(> 50mph)$ case is currently being investigated. Some oscillations due to gear shifting, are being observed in the velocity and position responses.

- Test 3: Varying time headway. See Figures 10(a) through 10(f).

A changing time headway profile, see Figure 10(f), is simulated using the following con-

stant PID gains:

$$k_1 = -0.3; \; k_2 = -4.0; \; k_3 = -0.0007$$

Good velocity tracking is achieved. As shown in Figure 10(a), the following vehicle speed will either lag behind or exceed the leading vehicle velocity for a short transient period. If the headway is increased during steady state, the position error becomes negative for a short time period, as expected, since the inter–vehicle spacing according to the previous time headway setting is below the desired value, see Figures 10(c), (d) and (f).

- Test 4: Effects of changing initial conditions. See Figures 11(a) through 11(f).

The effect of changing initial conditions was also investigated. The velocity reponse is shown in Figure 11(a). The following situation is considered: at time $t_1 = 150$ *sec*, the leading vehicle changes lanes and the new vehicle target is 10 *mph* faster and 10 *m* farther ahead than the previous one. The change in the measurement is therefore simulated as an instantaneous one. The results are quite satisfactory for both velocity and position tracking. The acceleration constraint is slightly exceeded due to the sudden change in the velocity and position measurements. This undesirable effect can be eliminated by choosing lower values for the position error limits in the PID controller shown in Figure 7(b).

- Test 5: Sampling frequency effect. See Figures 12(a) through 12(f).

All the previous simulations were performed for a 50 Hz controller sampling frequency. Figures 12(a)–(f) show the results obtained when the controller sampling frequency was changed to 20 Hz, and later on to 10 Hz. Little or no effect is noticed in this case.

Remark Since the vehicle dynamic in low speed is faster than that in high speed and the gains are designed mainly for high speed, the throttle, acceleration, and jerk exhibit oscillations in low speed. It is found that, in order to achieve good performance in both low and high speeds, one way is to use gain scheduling or adaptive gains.

5 Conclusion

In this report we designed an autonomous intelligent cruise controller for vehicle following under time headway policy. The controller was simulated using the longitudinal model of

the Lincoln Town car. Different tests were performed, including constant load disturbance, initial conditions and varying time headway effects. Good velocity and position tracking were achieved without violating the given driving comfort contraints.

References

[1] C. C. Chien and P. A. Ioannou, "Automatic Vehicle Following", *Proc. American Control Conference,* Chicago, IL, June 1992.

[2] Tom Xu, *Personal Communications.*

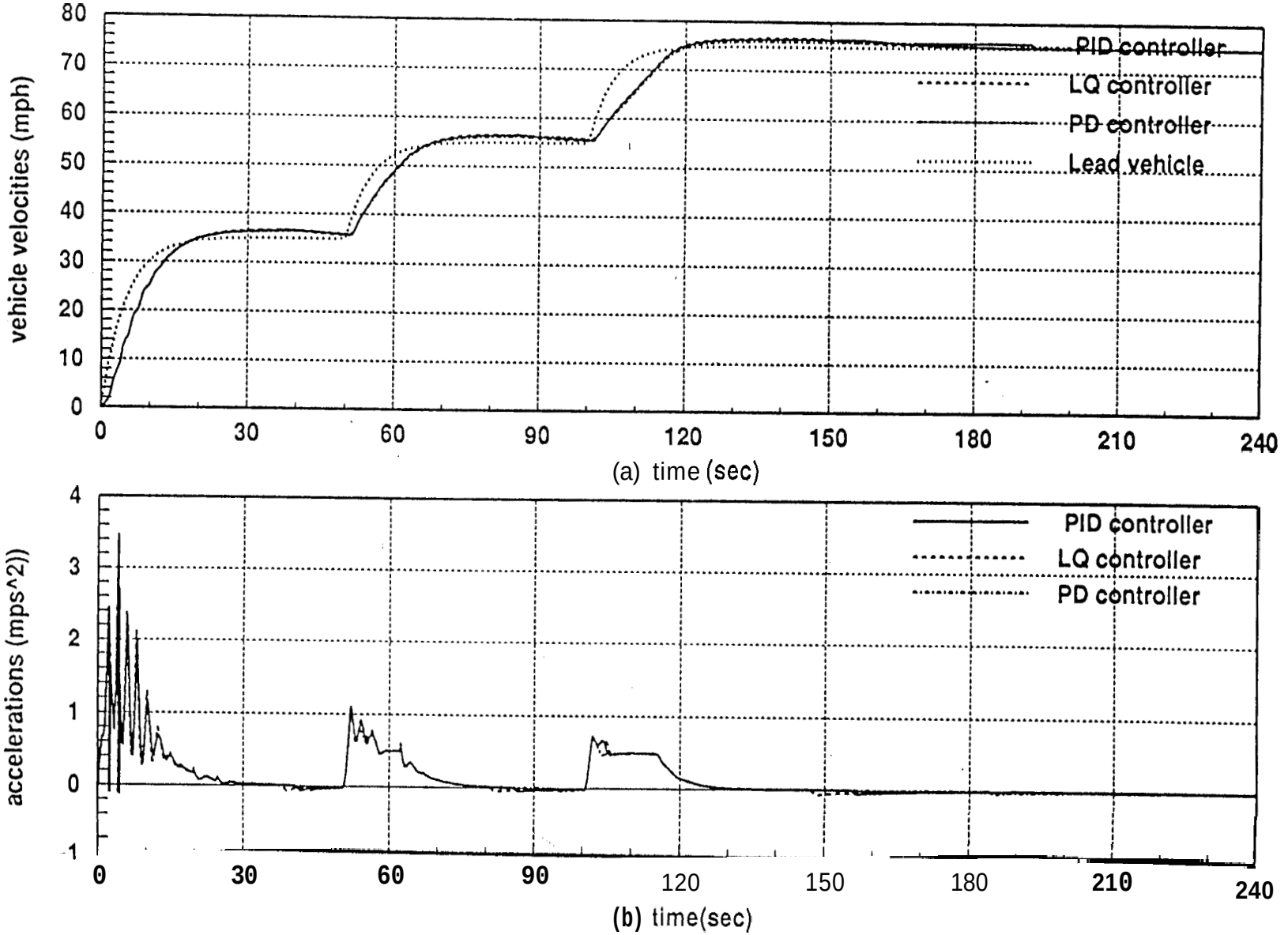

Figure 8: (a) Vehicle velocity vs. time, (b) Accelerations vs. time

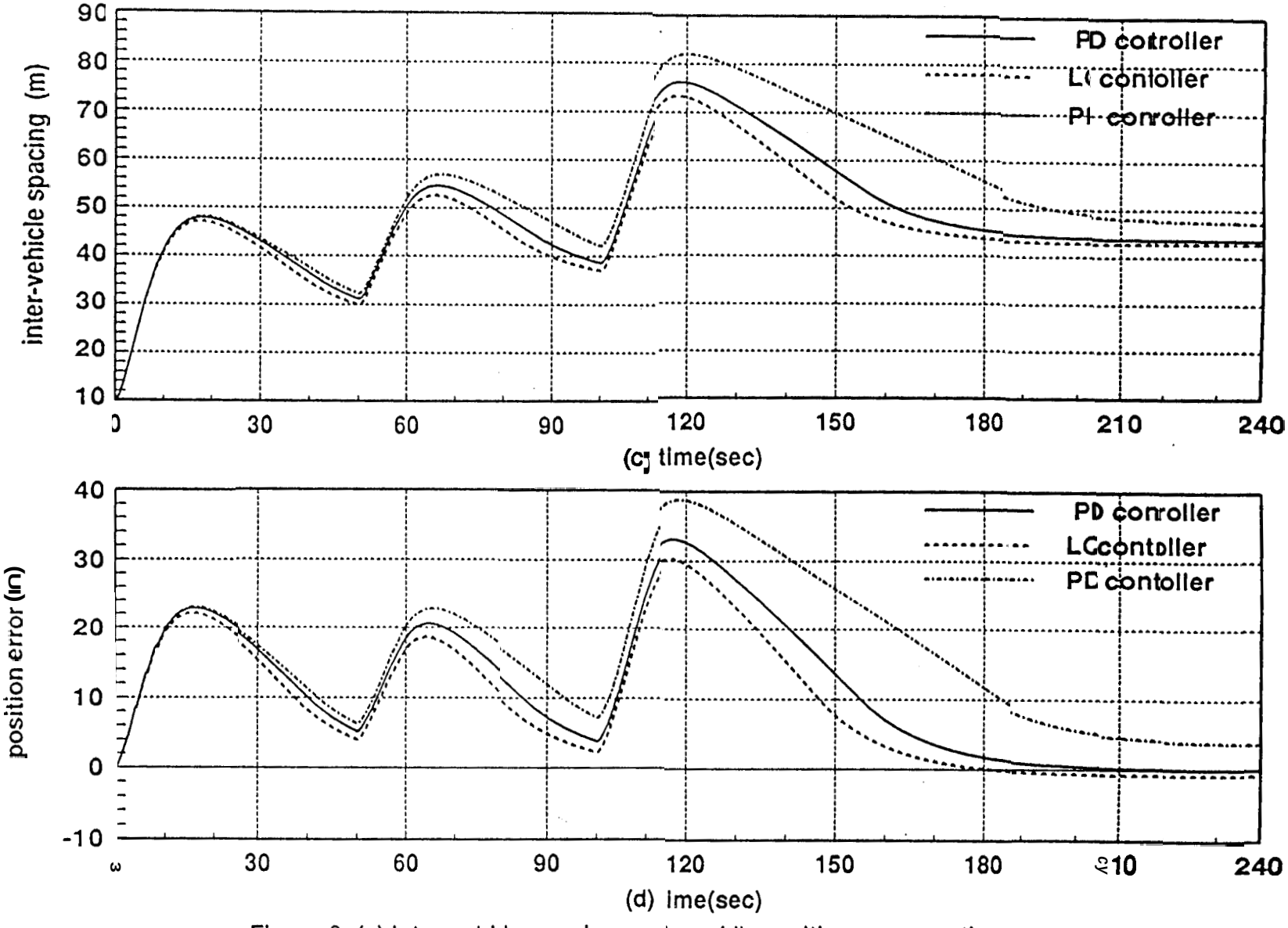

Figure 8: (c) Inter-vehide spacing vs. ime, (d) position error vs. time

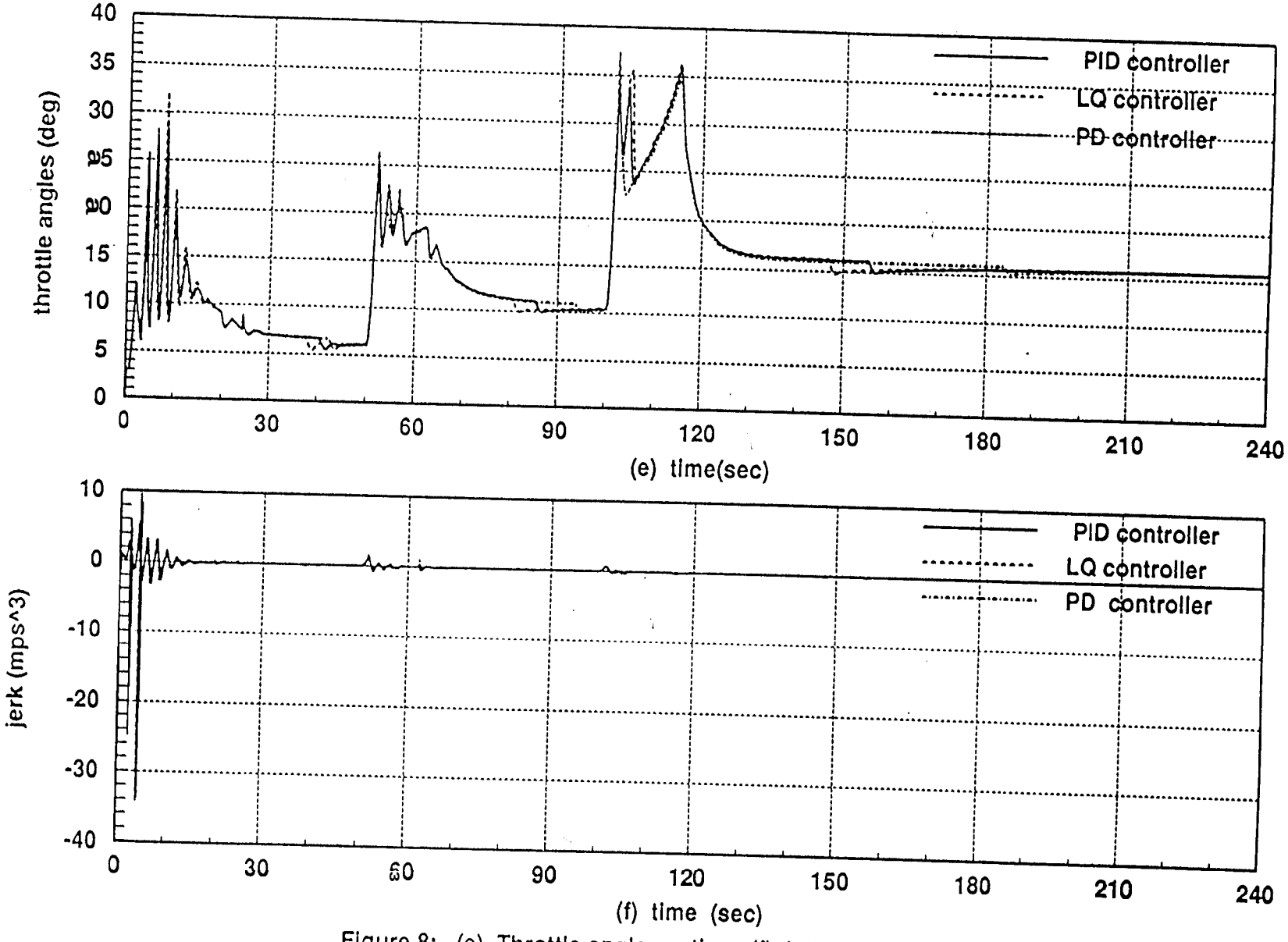

Figure 8: (e) Throttle angle vs. time, (f) Jerk vs. time

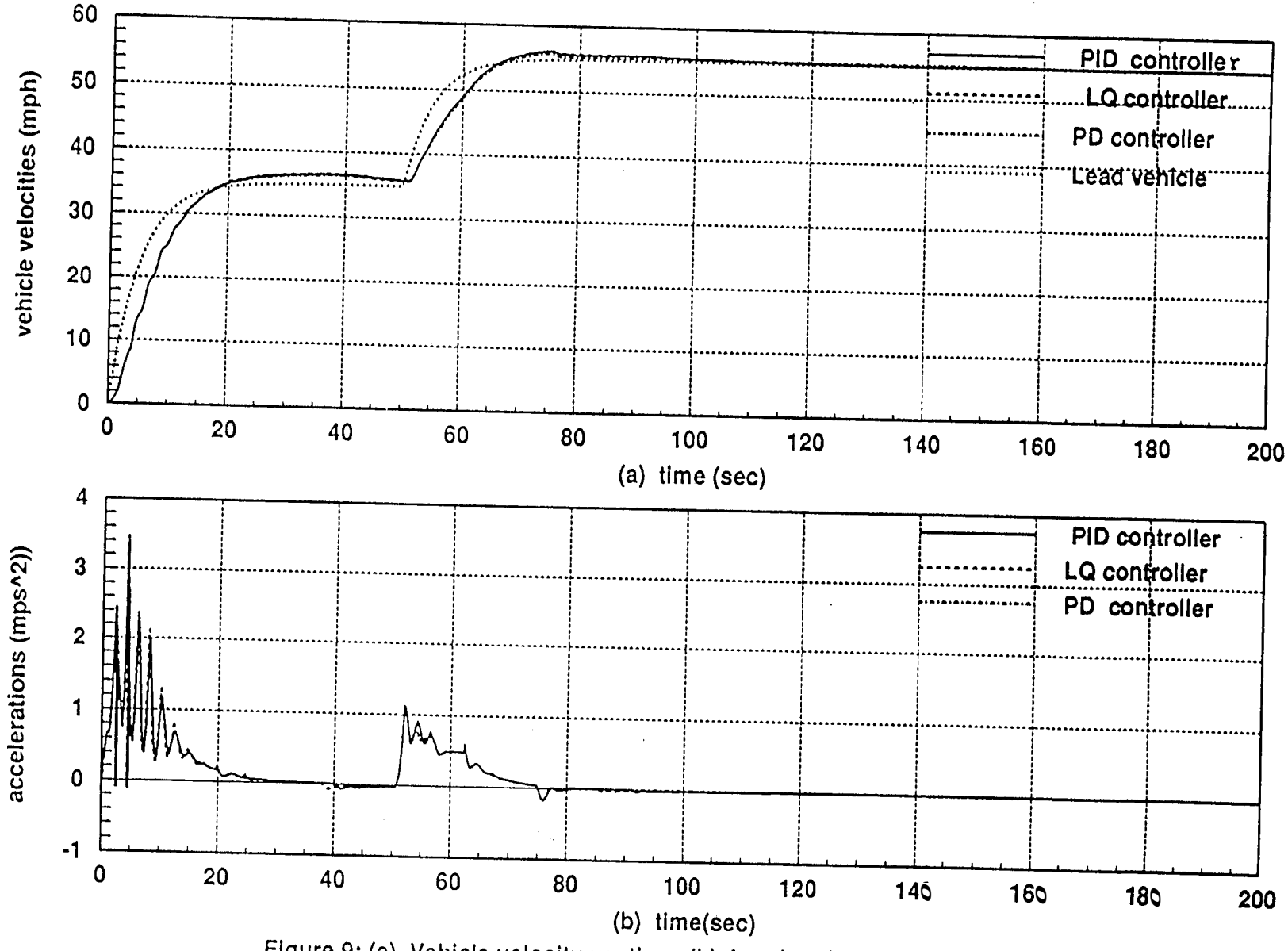

Figure 9: (a) Vehicle velocity vs. time, (b) Accelerations vs. time

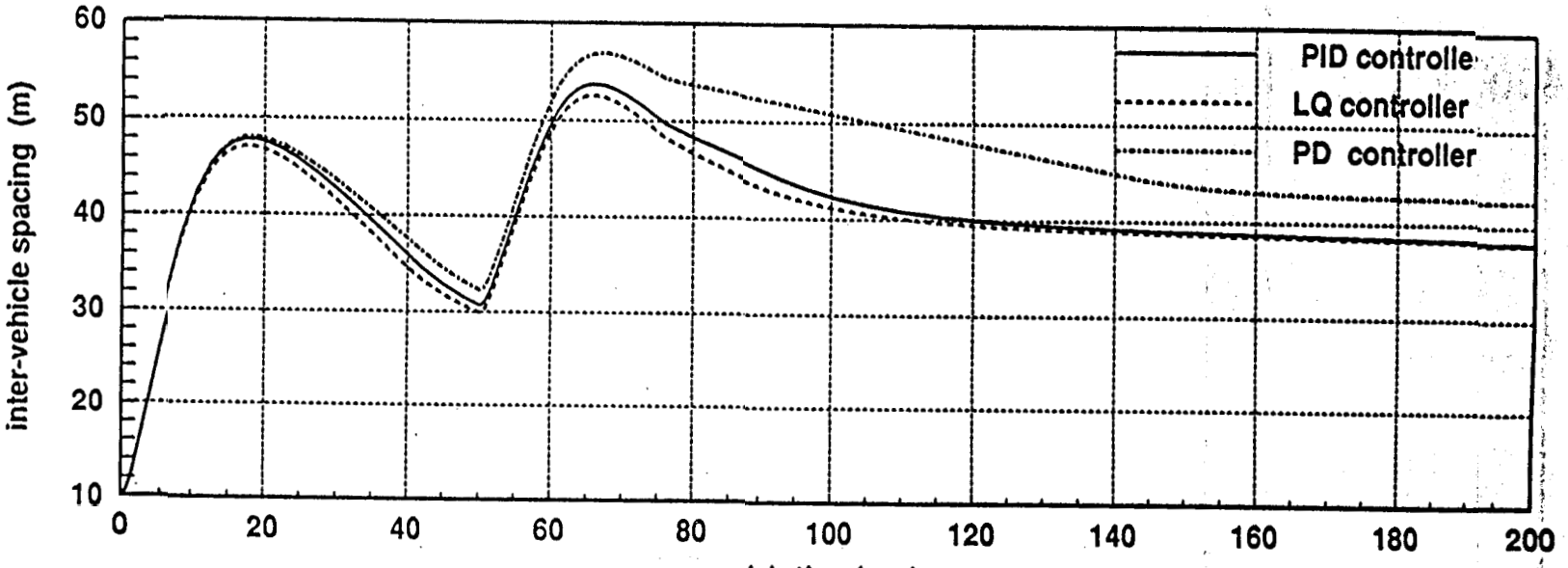

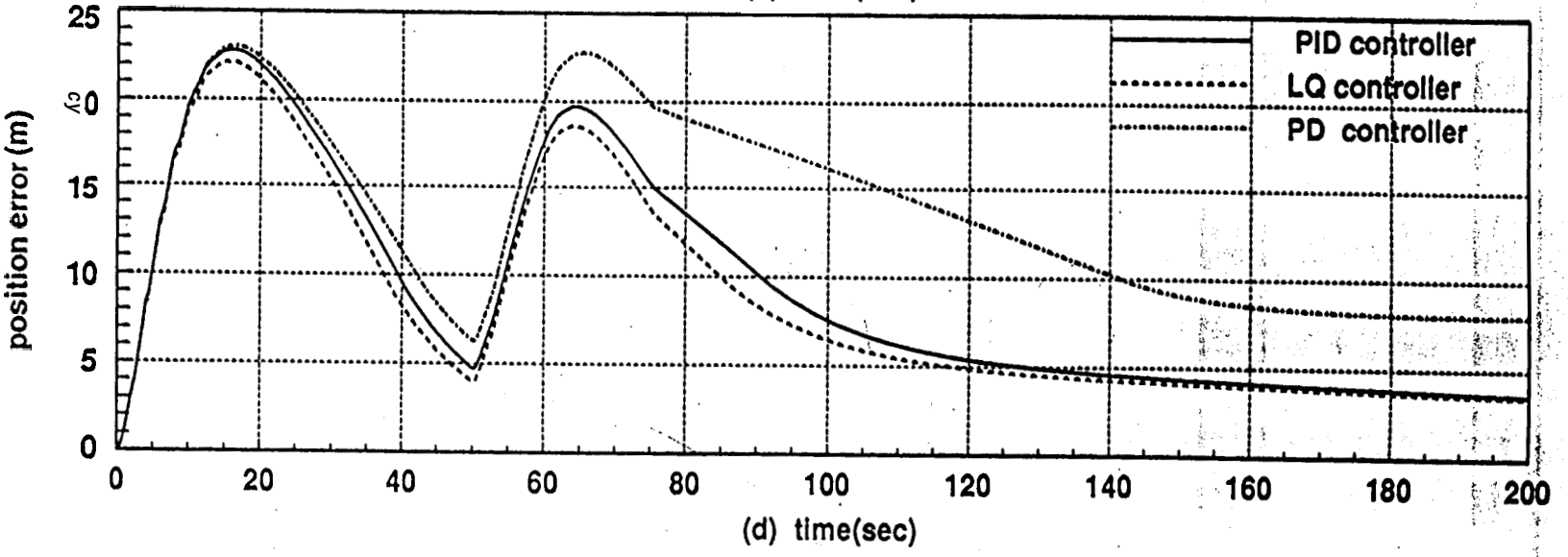

Figure 9: (c) Inter-vehicle position vs. time, (d) position error vs. time

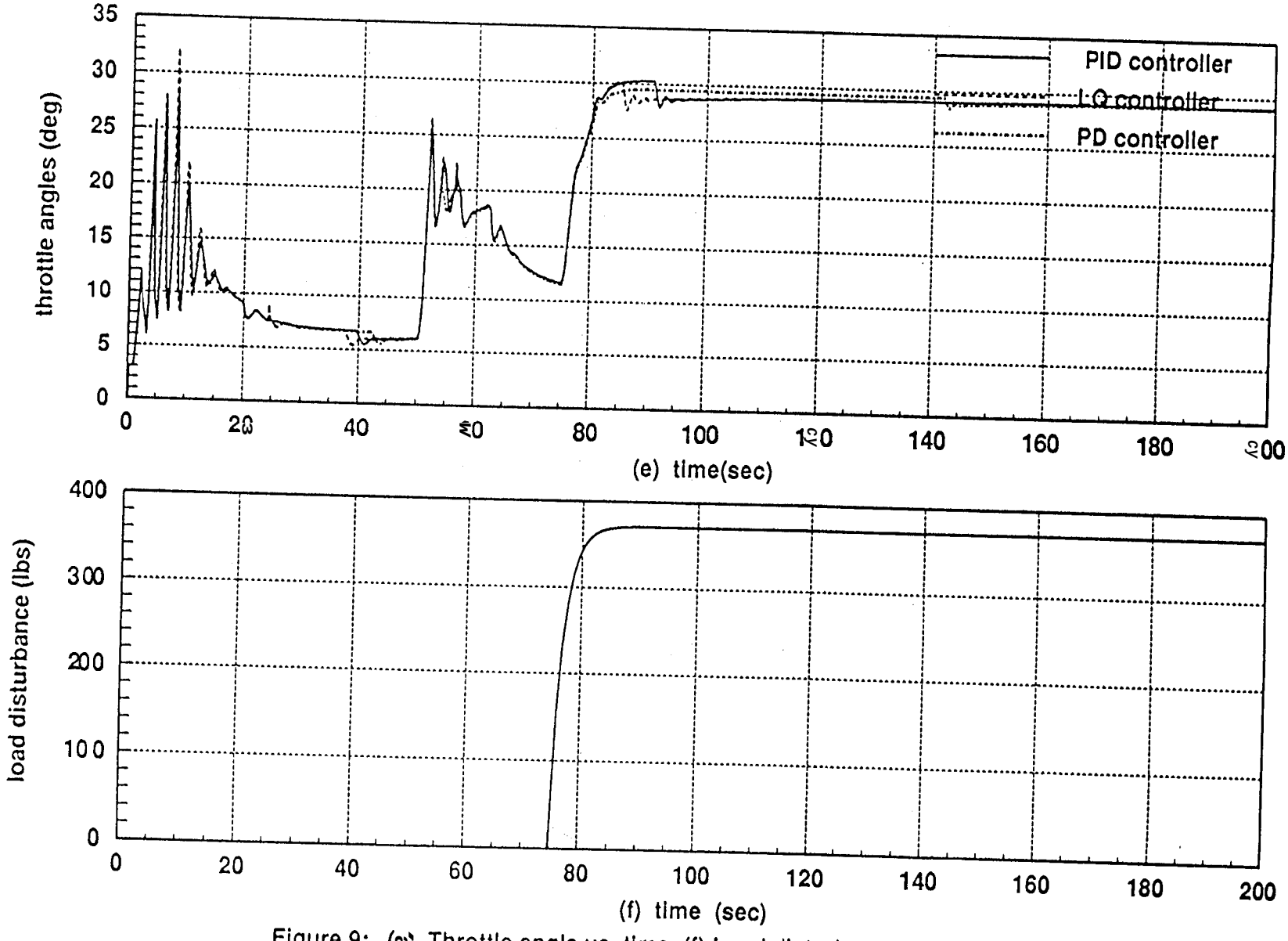

Figure 9: (e) Throttle angle vs. time, (f) Load disturbance vs. time

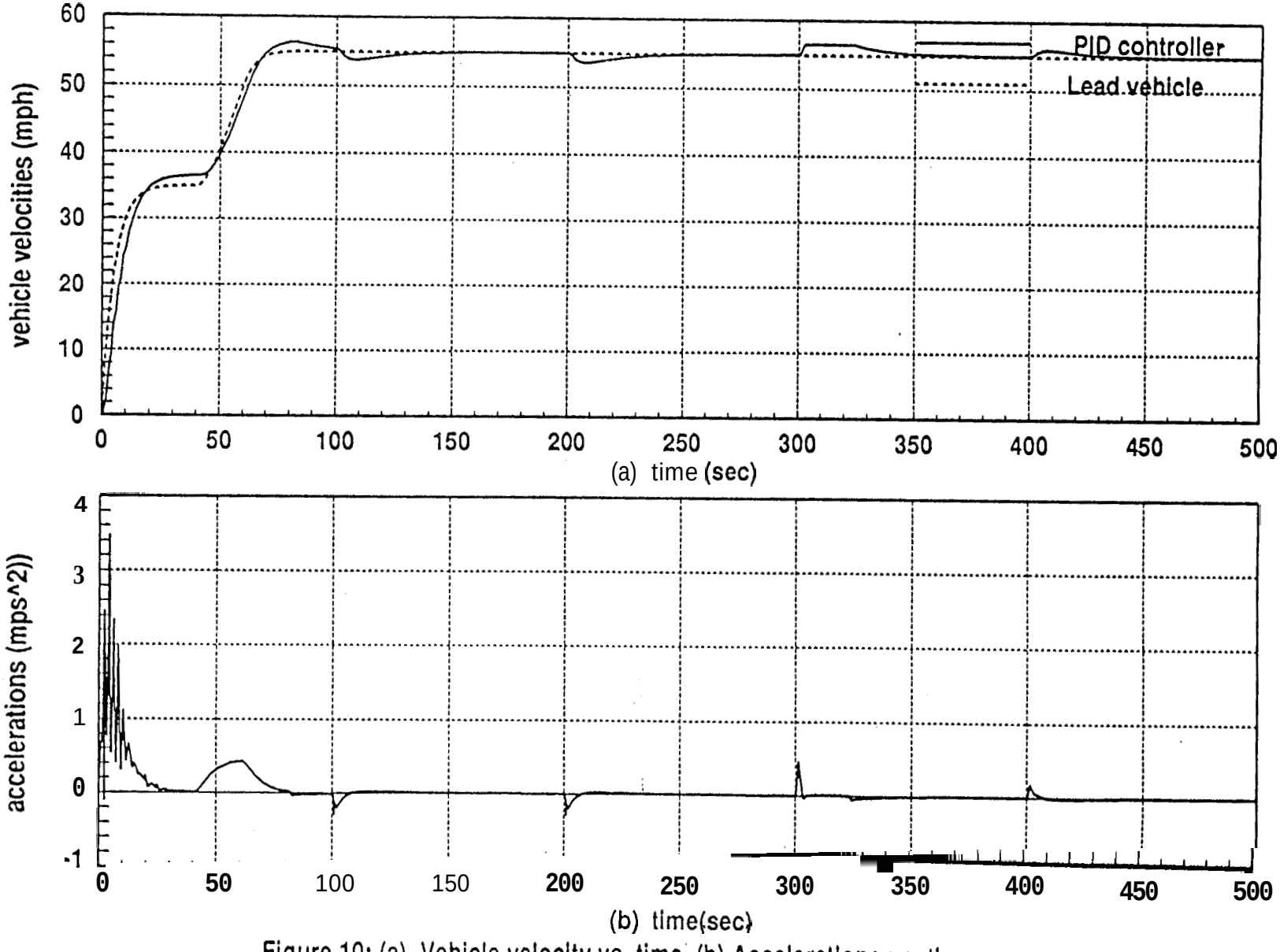

Figure 10: (a) Vehicle velocity vs. time, (b) Accelerations vs. time

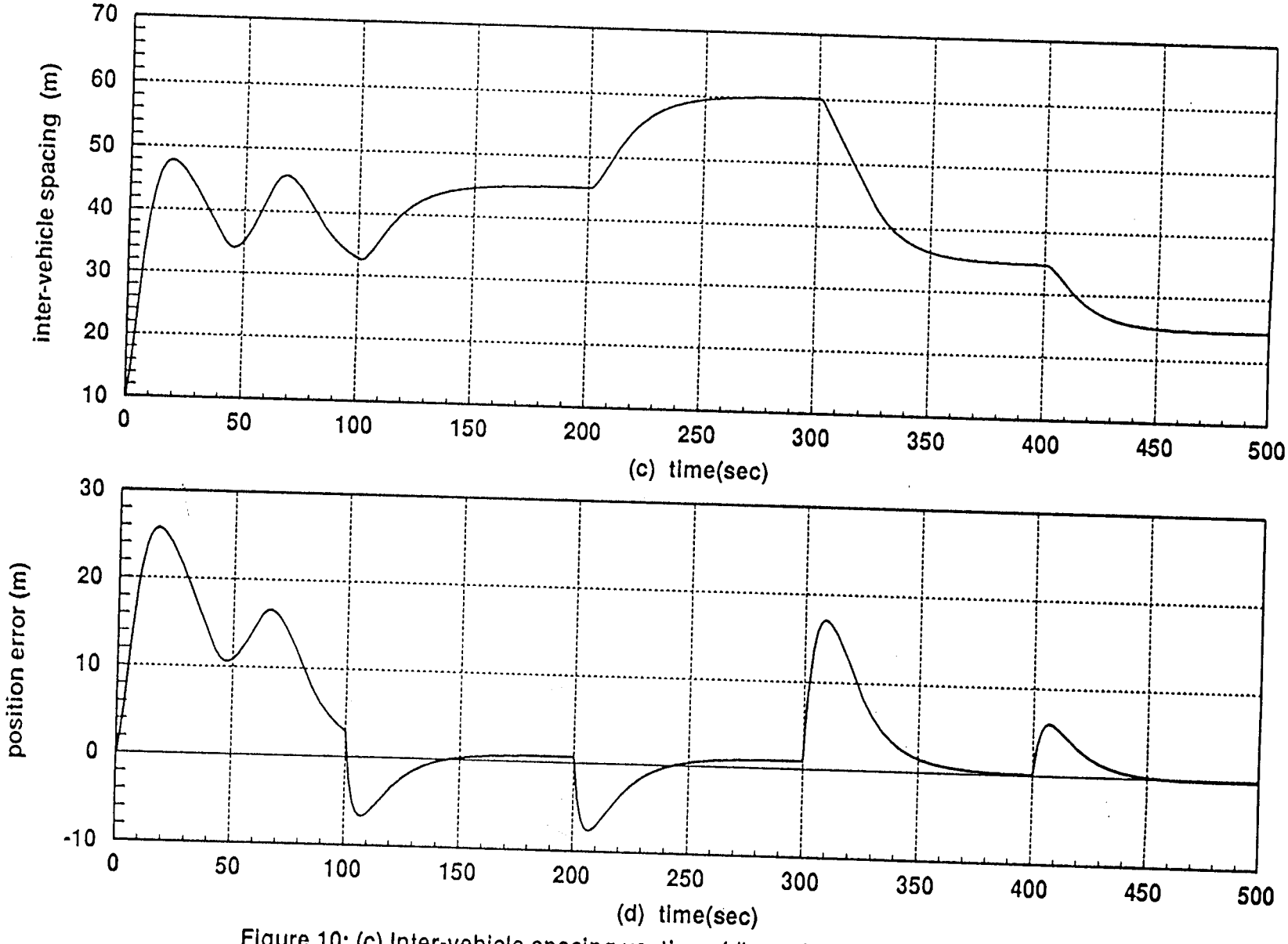

Figure 10: (c) Inter-vehicle spacing vs. time, (d) position error vs. time

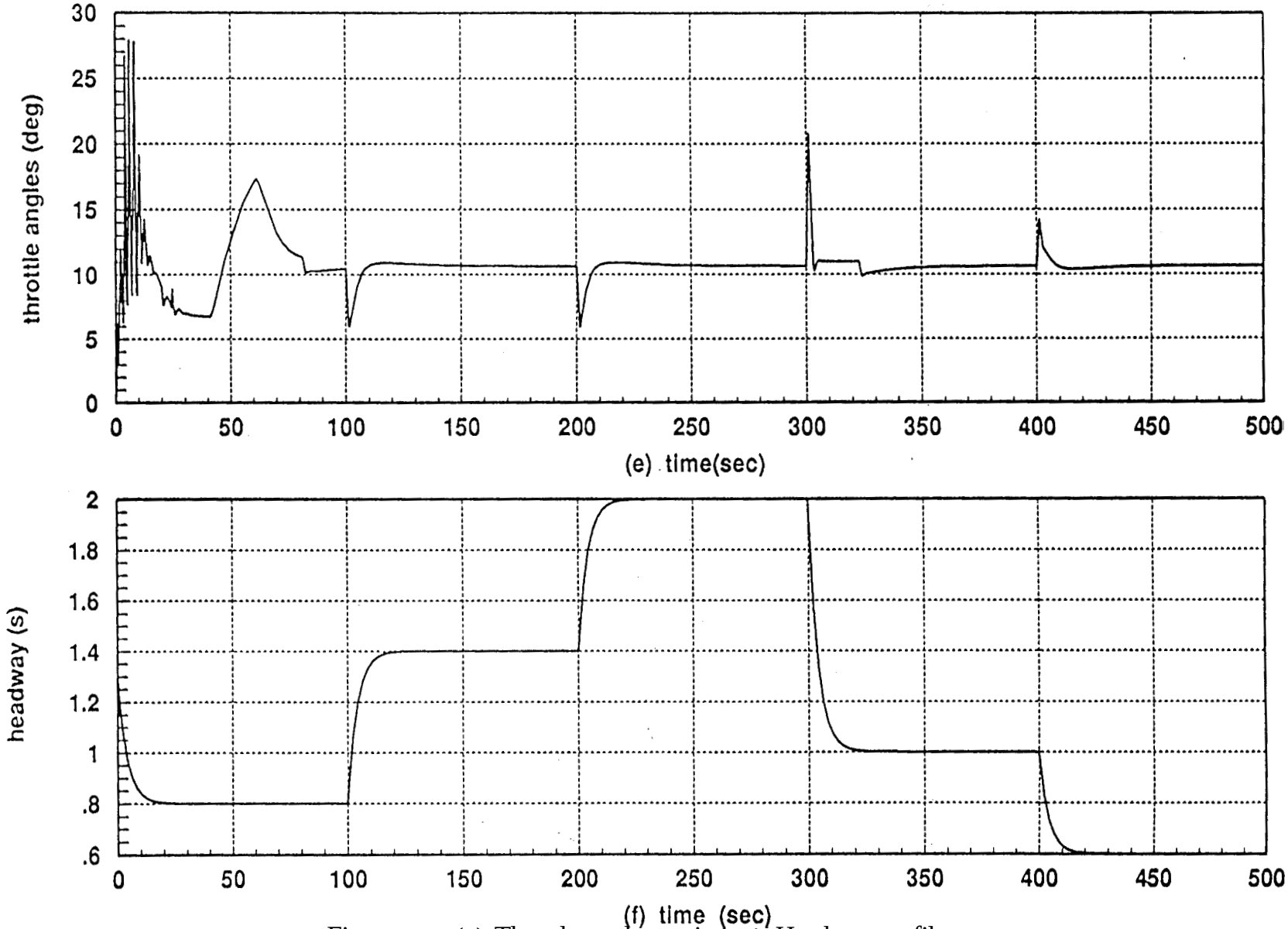

Figure 10: (e) Throttle angle **vs.** time, (f) Headway profile

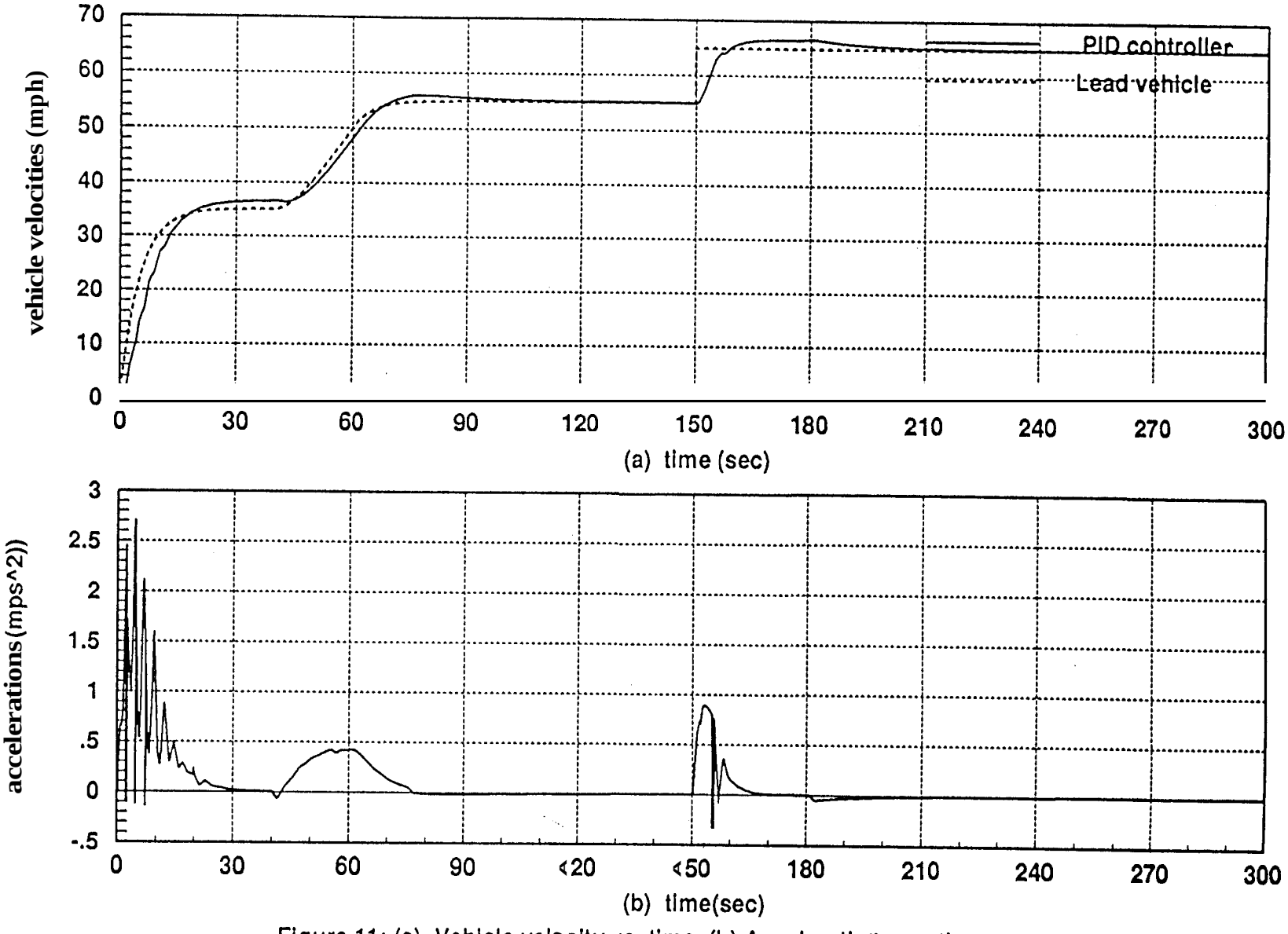

Figure 11: (a) Vehicle velocity vs. time, (b) Accelerations vs. time

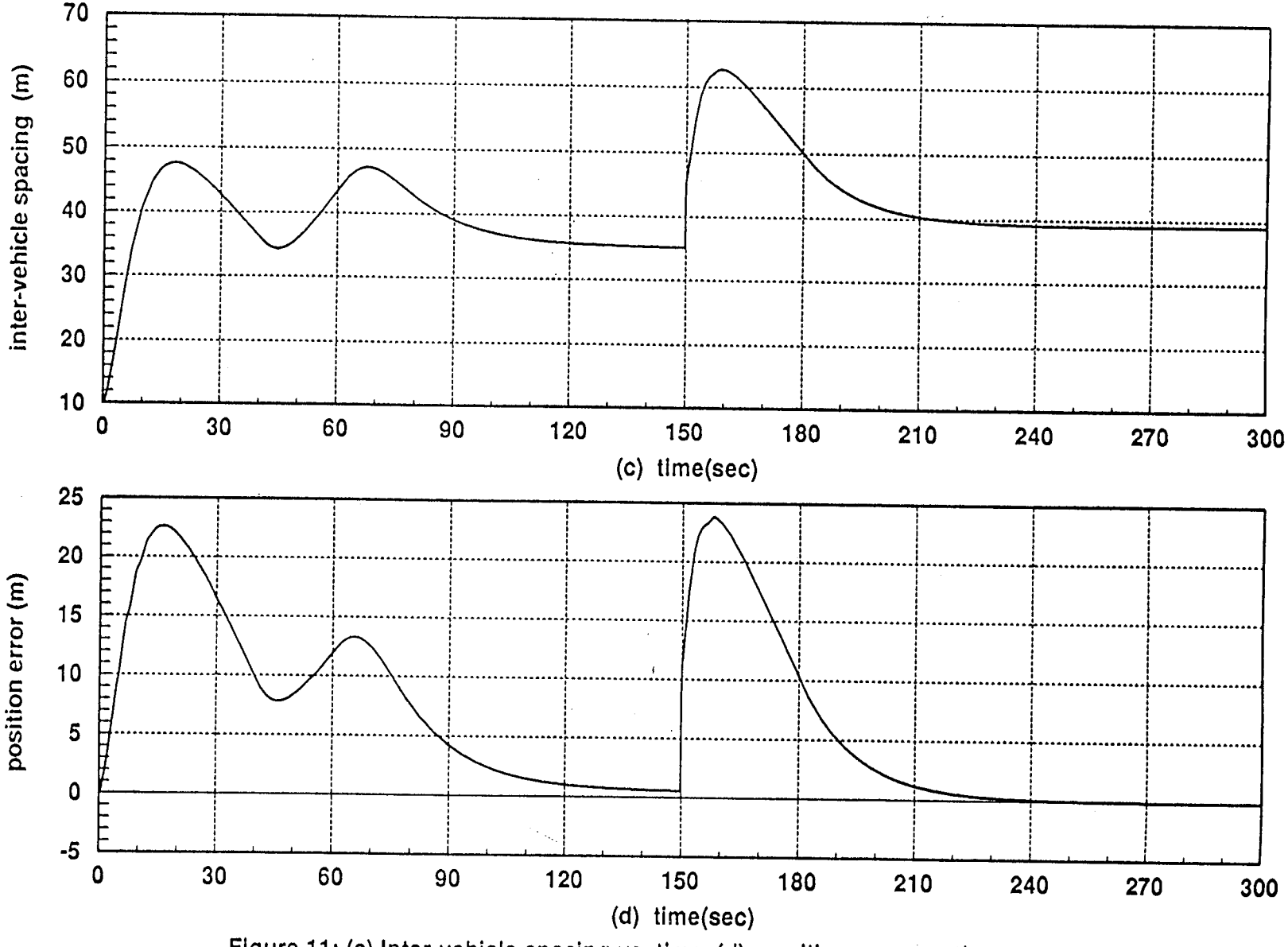

Figure 11: (c) Inter-vehicle spacing vs. time, (d) position error vs. time

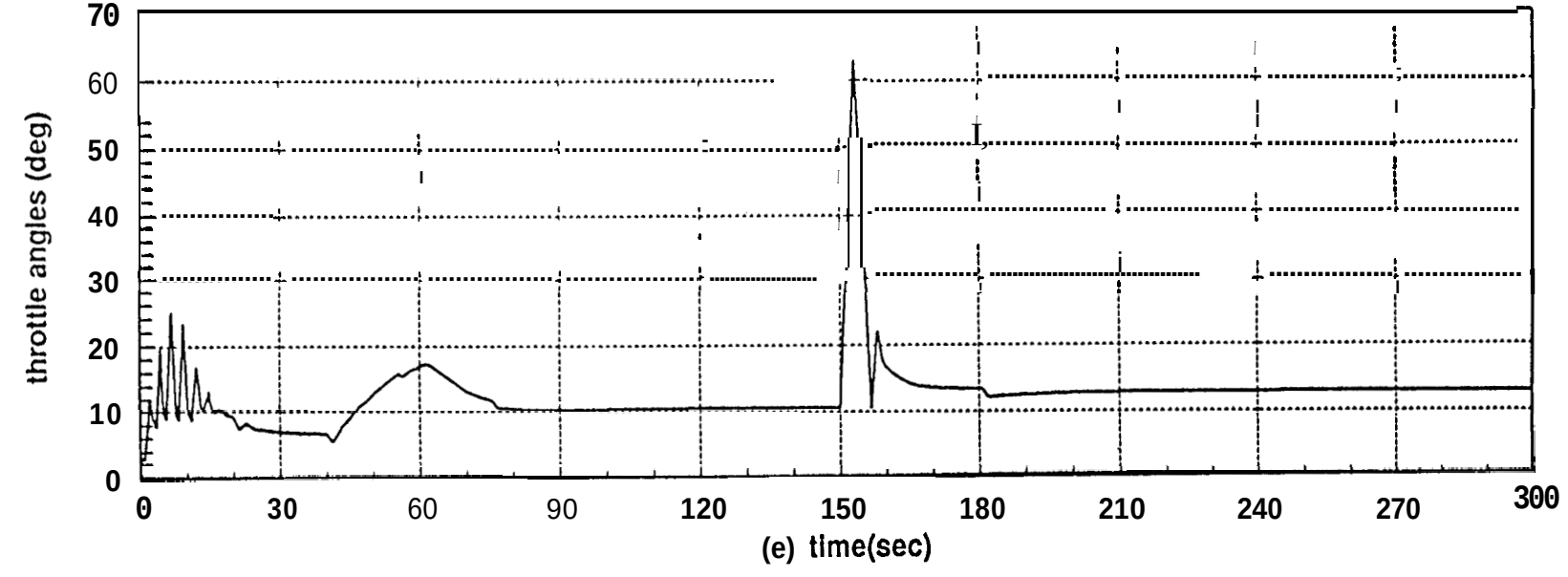

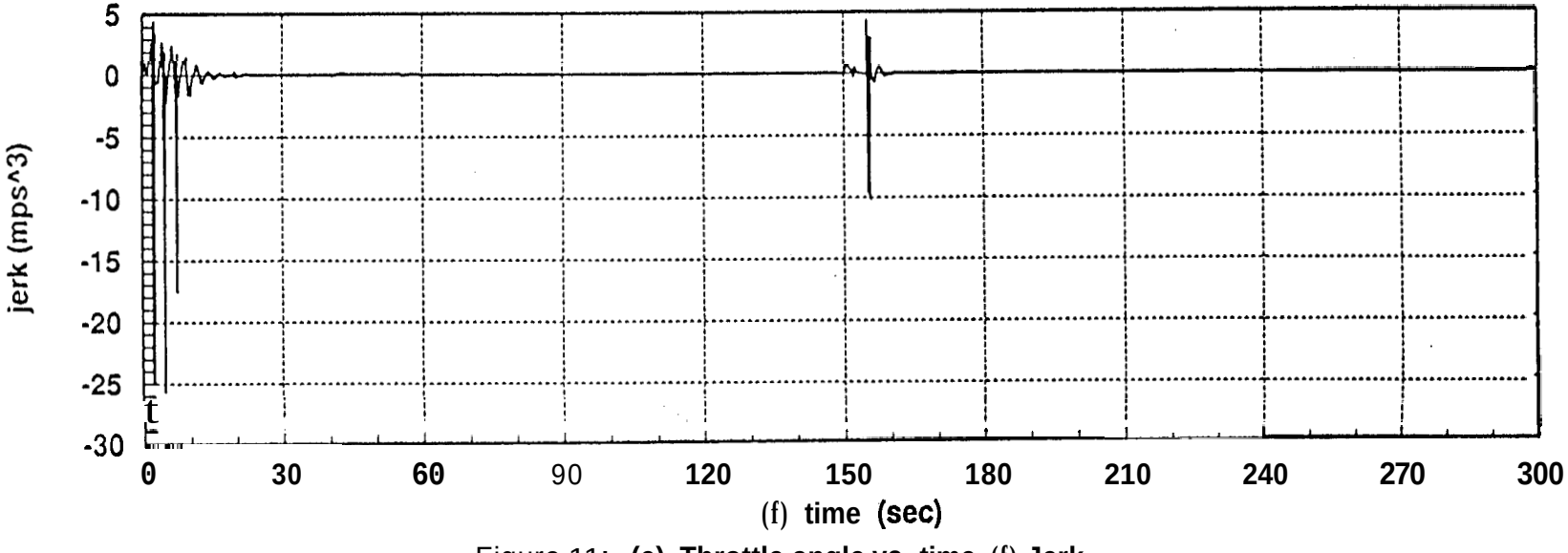

Figure 11: **(e) Throttle angle vs. time,** (f) **Jerk**

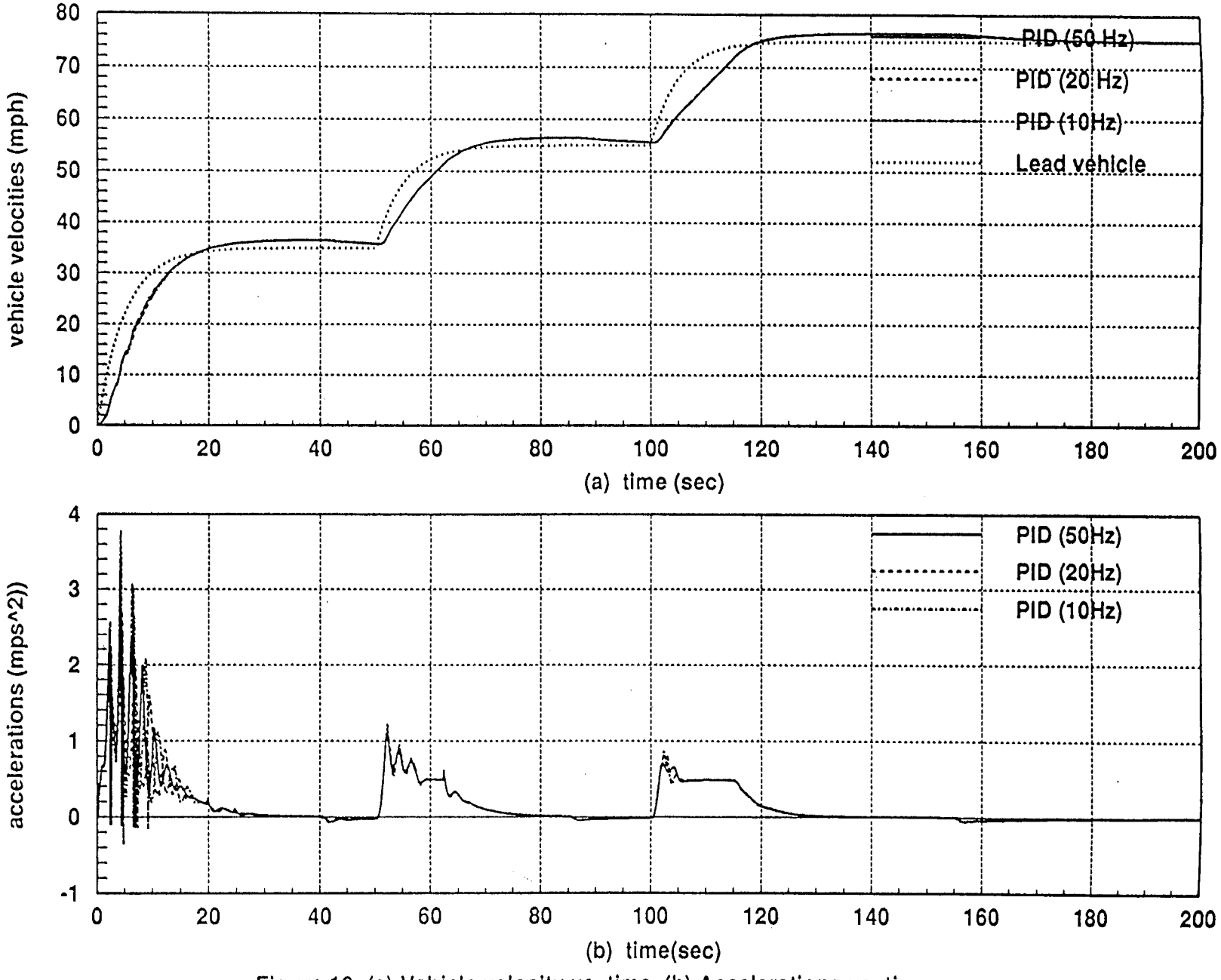

Figure 12: (a) Vehicle velocity vs. time, (b) Accelerations vs. time

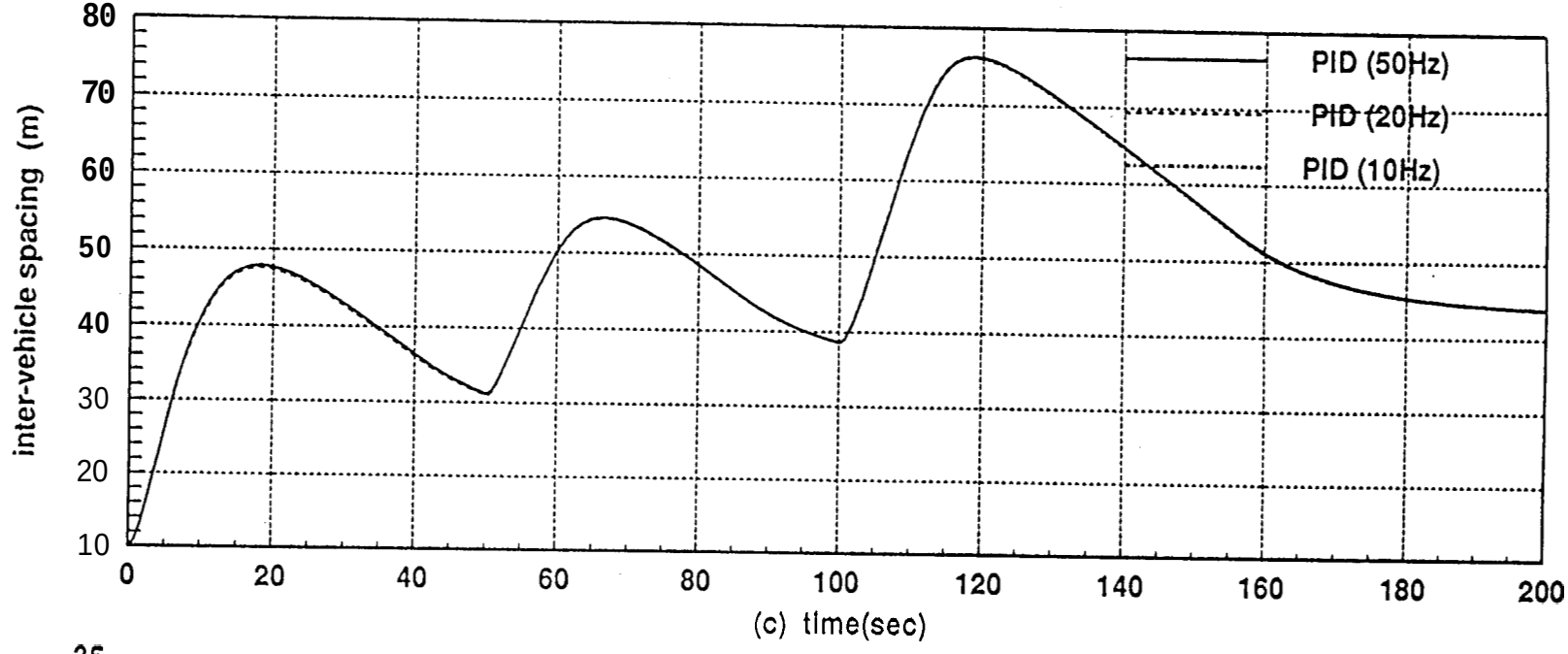

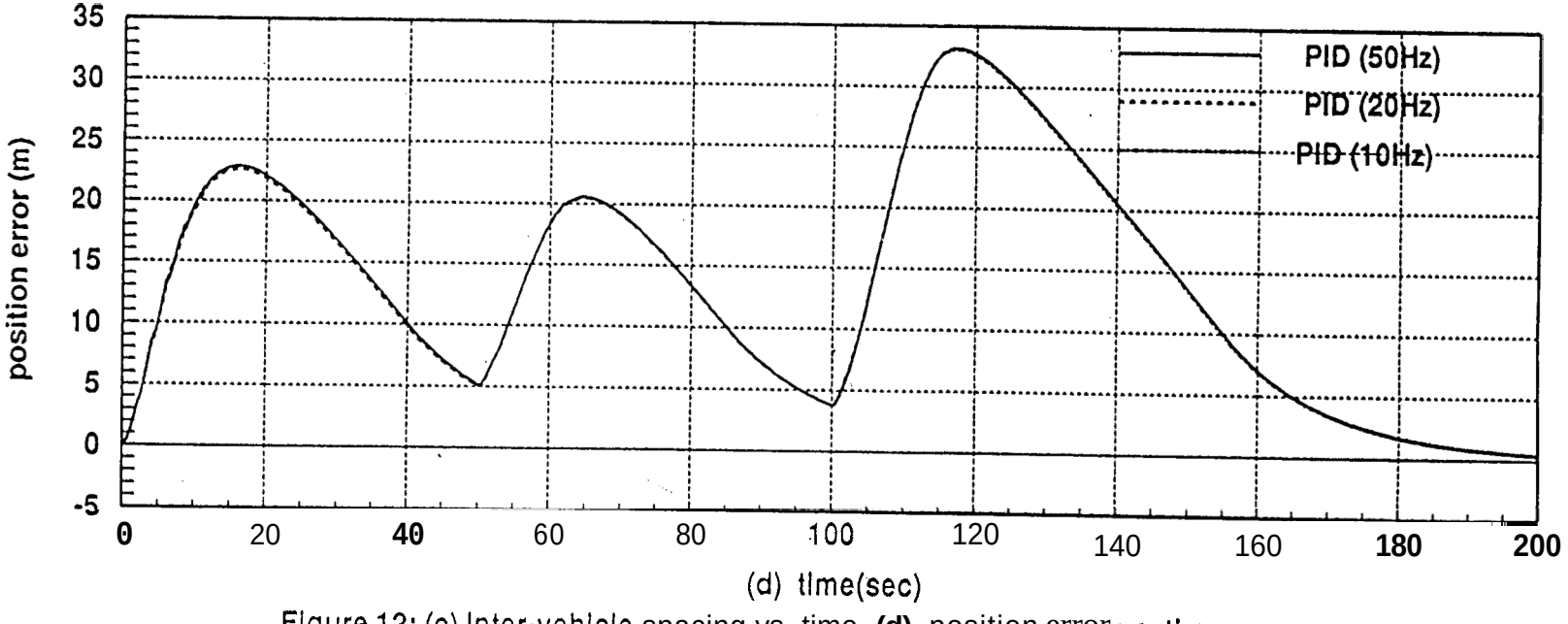

Figure 12: (c) Inter-vehicle spacing vs. time, **(d)** position error **vs. time**

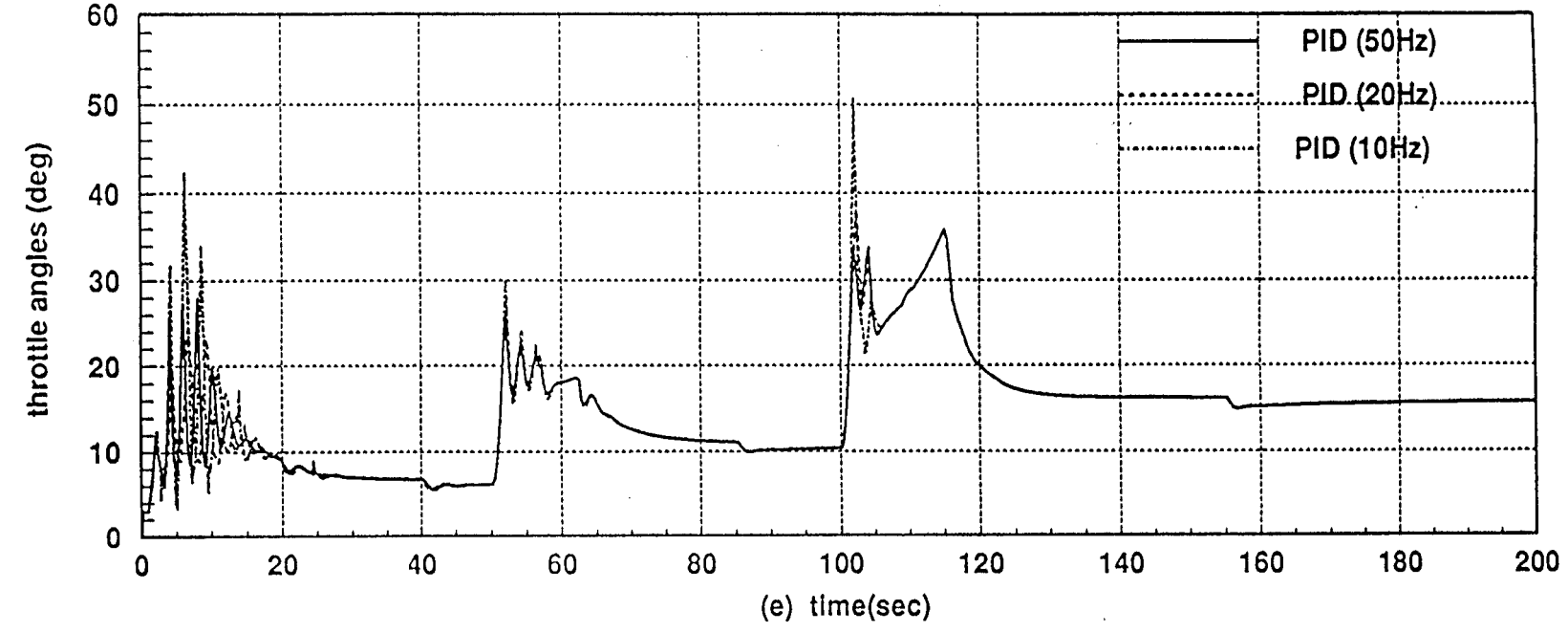

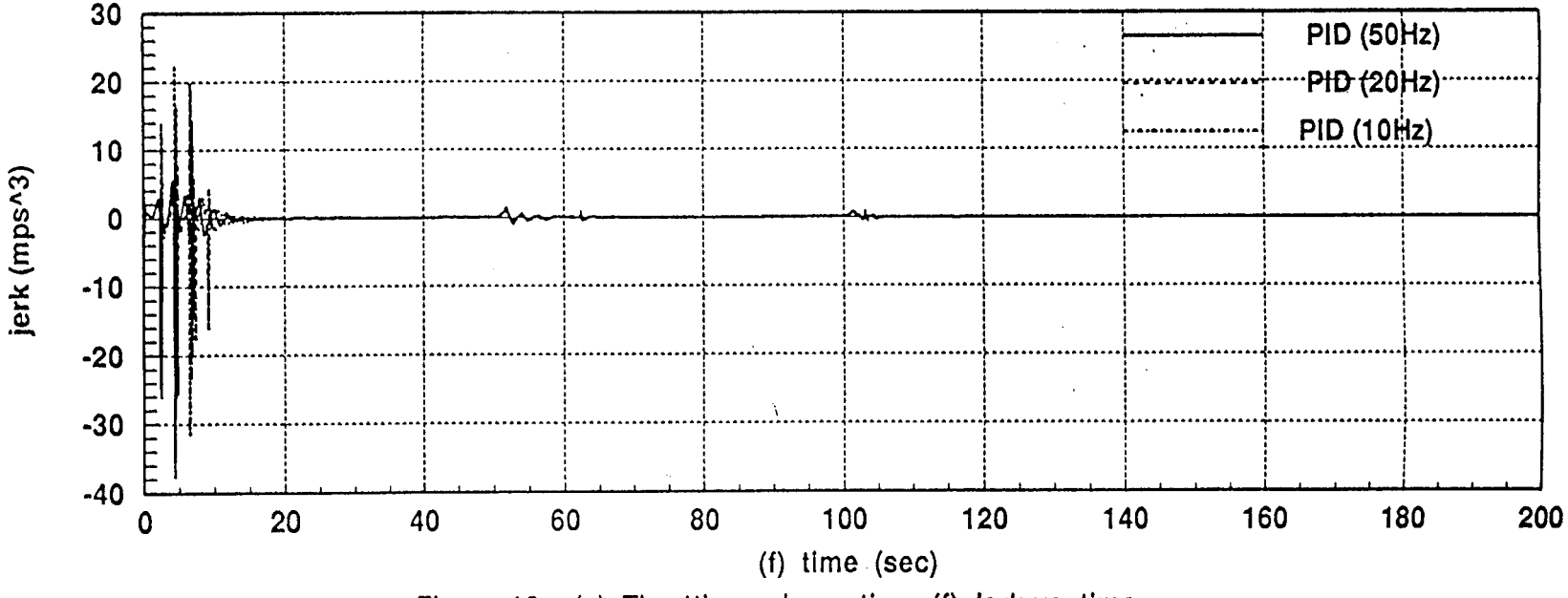

Figure 12: (e) Throttle angle vs. time, (f) Jerk vs. time